Antoni SAWICKI

Politechnika Częstochowska, Instytut Elektroenergetyki

Assessement of power parameters of asymmetric arcs by means of the Cassie and Mayr models

***Abstract**. Kinds of arc asymmetry have been classified. Factors influencing such asymmetry have been given. Cassie and Mayr models of asymmetric arc have been developed with implementation in MATLAB-Simulink application. Energetic properties of these models have been presented based on simulation results of arc powered by sinusoidal and square current.*

***Streszczenie.** Dokonano klasyfikacji rodzajów asymetrii łuku. Podano czynniki wpływające na tą asymetrię. Opracowano modele Cassiego i Mayra łuku asymetrycznego. Przedstawiono implementacje modeli łuku asymetyrycznego w programie MATLAB-Simulink. Na podstawie wyników symulacji łuku zasilanego prądem sinusoidalnym i prostokątnym zaprezentowano właściwości energetyczne tych modeli (**Ocena właściwości energetycznych łuku asymetrycznego za pomocą modeli Cssiego i Mayra**).*

Keywords: Cassie model, Mayr model, asymmetric arc model.
Słowa kluczowe: model Cassiego, model Mayra, model łuku asymetrycznego.

Introduction

The AC arc has been used in welding and other metallurgical technologies for an extended period of time due to its numerous advantages and relatively low cost [1]. Also in lighting technology with high pressure discharge lamps powering the application of AC arcs is widespread. In the analyses of electromagnetic and thermal processes in arc and plasma devices the asymmetry of the dynamic voltage-current characteristics is typically disregarded, as it is usually small. In some devices and under some operating conditions, however, the asymmetry is significant and may generate even harmonics, the constant component of the current saturating magnetic cores and causing electrolysis. There exist a number of factors potentially causing the asymmetry of the dynamic and static arc characteristics [2, 3]. Some of them are shown in Table 1.

Table 1. Factors affecting the asymmetry type in an electrical arc

Factor type	Arc asymmetry type	
	Electrode	Column
Material	The two electrodes made of materials of different emission properties.	Periodical constrictions of the conical column part near the cathode.
Mechanical	Rotating drum or disc electrodes with inserts made of materials of different emission properties; insertion of micro-particles into the hollow cathode.	Relative periodical movements of electrodes cause variation of the arc length; relative periodical movement of the diaphragm dividing the arc; relative periodical movement of the discharge channel or chamber; insertion of micro-particles into the column.
Acoustic	Periodical gas pressure alterations inside the hollow cathode	Periodical gas pressure alterations in the discharge channel or chamber.
Magnetic	Periodical shifts of electrode spots towards the materials of different emission properties.	Periodical deviations of the arc column.
Electrical	Periodical alterations of the split electrode current [3, 4]	Periodical alterations of the auxiliary electrode current in a multi-arc system [4]
Ionization	Periodical shifts of electrode spots towards the materials of different emission properties..	Periodical deviations of the arc column; periodical alterations in the plasma ionization.

The dynamic characteristics of an electrical arc is represented as

(1) $$u_a = \pm\alpha + u_{col}(i)$$

where: α - is the sum of voltage drops near the electrodes ($\alpha = U_C + U_A$); u_{col} – is the voltage drop at the plasma arc column. Another form of the equation also indicates the risk of asymmetry

(2) $$u_a = \alpha + \beta L$$

where: β – is the voltage gradient; L – is the distance between the electrodes. Periodical and synchronous with the current alternations of any of these quantities cause asymmetry

- electrode asymmetry

(3) $$u_a = \alpha(sign(i)) + \beta L$$

- or column asymmetry

(4) $$u_a = \alpha + \beta(sign(i))L$$

or

(5) $$u_a = \alpha + \beta L(sign(i))$$

Modeling the asymmetric arc

If the asymmetry of the arc electrical characteristics follows from the dependence of the voltage drops near the electrodes on the current flow direction, then it can be represented as

(6) $$u_a = \begin{cases} -\alpha_1 + u_{col}(i), & \text{if } i < 0 \\ \alpha_2 + u_{col}(i), & \text{if } i \geq 0 \end{cases}$$

The arc model equation can be obtained from the heat balance

(7) $$P_{el} = ui = P_{dis} + \frac{dH}{dt}$$

where: H – is the plasma enthalpy; P_{el} – is the supplied electrical power; P_{dis} – is the dissipated heat power. The phenomenon of energy dissipation occurs both in the regions near the electrodes P_{AC}, and in the plasma column P_{col}

(8) $$P_{dis} = P_{AC} + P_{col} = (\alpha + u_{col})i$$

If the plasma column is periodically distorted, then the dissipated power is also subject to periodical changes and does not meet the symmetry condition during a half-period:

(9) $$\begin{gathered} P_{dis}(t) = \begin{cases} i \cdot u_{col1}(i), & if\ i < 0 \\ i \cdot u_{col2}(i), & if\ i \geq 0 \end{cases} \\ P_{dis}(t) = P_{dis}(t+T) \\ P_{dis}(t) \neq P_{dis}(t+0{,}5T) \end{gathered}$$

The modified differential equation of the Cassie asymmetric arc model [5] can be represented as

(10) $$\frac{1}{g}\frac{dg}{dt} = \frac{1}{\theta_C}\left[\frac{u_{col}^2}{U_C^2(i)} - 1\right]$$

or

(11) $$\frac{1}{r}\frac{dr}{dt} = \frac{1}{\theta_C}\left[1 - \frac{u_{col}^2}{U_C^2(i)}\right]$$

where: is the time constant of the Cassie model

(12) $$\theta_C = \frac{h}{\Delta P}$$

is the voltage in the Cassie model

(13) $$U_C^2 = \frac{l}{\sigma}\Delta P$$

h – is the surface density of the plasma enthalpy; l – is the arc length; σ - is the plasma conductivity; ΔP – is the surface density of the dissipated power.

The value of the amplitudes in the Cassie function are defined by the formulas:

(14) $$U_{C\min} = \sqrt{\frac{l_{\min}}{\sigma}\Delta P}$$

(15) $$U_{C\max} = \sqrt{\frac{l_{\max}}{\sigma}\Delta P}$$

or

(16) $$U_{C\min} = \sqrt{\frac{l}{\sigma_{\max}}\Delta P}$$

(17) $$U_{C\max} = \sqrt{\frac{l}{\sigma_{\min}}\Delta P}$$

The asymmetric characteristics of the Cassie voltage can be approximated by means of [5]:
- the step function

(18) $$U_C(i) = U_{C\min}\frac{sign(-i)+1}{2} + U_{C\max}\frac{sign(i)+1}{2}$$

- the unipolar sigmoid function

(19) $$U_C(i) = U_{C\min} sigmu(-i) + U_{C\max} sigmu(i)$$

where

(20) $$sigmu(i) = \frac{1}{1+e^{-\beta i}}, \ \beta > 0$$

- the bipolar sigmoid function

(21) $$U_C(i) = 0{,}5\Delta U_C \cdot sigmb(i) + q$$

where

(22) $$sigmb(i) = \frac{1-e^{-\beta i}}{1+e^{-\beta i}}, \ \beta > 0$$

$$\Delta U_C = U_{C\max} - U_{C\min}, \ q = U_{C\max} - 0{,}5\Delta U_C.$$

In the boundary inertia-free case ($\theta_C \to 0$) it is possible to obtain from the asymmetric arc models (10) and (11) the required static arc characteristics

(23) $$u_{col}(i) = u_C(i) = U_{C\min}\frac{sign(-i)+1}{2} + U_{C\max}\frac{sign(i)+1}{2}$$

or

(24) $$u_{col}(i) = u_C(i) = U_{C\min} sigmu(-i) + U_{C\max} sigmu(i)$$

or

(25) $$u_{col}(i) = u_C(i) = 0{,}5\Delta U_C \cdot sigmb(i) + q$$

The Mayr mathematical models of the asymmetric arc [6] can be represented in
the conductance form

(26) $$\frac{1}{g}\frac{dg}{dt} = \frac{p_M(i)}{H_0}\left[\frac{u_{col}i}{p_M(i)} - 1\right]$$

or

(27) $$\frac{1}{g}\frac{dg}{dt} = \frac{p_M(i)}{H_0}\left[\frac{i^2}{g p_M(i)} - 1\right]$$

or the resistance form

(28) $$\frac{1}{r}\frac{dr}{dt} = \frac{p_M(i)}{H_0}\left[1 - \frac{u_{col}i}{p_M(i)}\right]$$

or

(29) $$\frac{1}{r}\frac{dr}{dt} = \frac{p_M(i)}{H_0}\left[1 - \frac{i^2 r}{p_M(i)}\right]$$

and the Mayr powers can be obtained from the two equations below

$$P_{M\min} = U_{01} I_{01} \tag{30}$$

$$P_{M\max} = U_{02} I_{02} \tag{31}$$

where: H_0 is the plasma enthalpy; (U_{01}, I_{01}), (U_{02}, I_{02}) – are the coordinates of the two points from among the points belonging to the two branches of the static voltage-current characteristics of the arc.

The Mayr asymmetric power characteristics can be approximated by [6]:

- the step function

$$P_M(i) = P_{M\min} \frac{sign(-i)+1}{2} + P_{M\max} \frac{sign(i)+1}{2} \tag{32}$$

- the unipolar sigmoid function

$$P_M(i) = P_{M\min} sigmu(-i) + P_{M\max} sigmu(i) \tag{33}$$

where

$$sigmu(i) = \frac{1}{1+e^{-\beta i}}, \quad \beta > 0; \tag{34}$$

- the bipolar sigmoid function

$$P_M(i) = 0{,}5 \Delta P_M \cdot sigmb(i) + q \tag{35}$$

where:

$$sigmb(i) = \frac{1-e^{-\beta i}}{1+e^{-\beta i}}, \quad \beta > 0; \tag{36}$$

$$\Delta P_M = P_{M\max} - P_{M\min}, \; q = P_{M\max} - 0{,}5 \Delta P_M .$$

Since the time constant is associated with the Mayr model power

$$\theta_M(i) = \frac{H_0}{p_M(i)} \tag{37}$$

where

$$p_M(i) = \begin{cases} P_{M\min}, & \text{if} \quad i < 0 \\ P_{M\max}, & \text{if} \quad i \geq 0 \end{cases} \tag{38}$$

the time constant alteration range is obtained

$$\theta_M(i) = \begin{cases} \theta_{M\max} = \dfrac{H_0}{P_{M\min}}, & \text{if} \quad i < 0 \\ \theta_{M\min} = \dfrac{H_0}{P_{M\max}}, & \text{if} \quad i \geq 0 \end{cases} \tag{39}$$

In the boundary inertia-free case ($\theta_M \to 0 \Rightarrow H_0 \to 0$) it is possible to obtain from the asymmetric arc models (26)-(29) the required static characteristics

$$\begin{aligned} -u_{col}(i) &= \frac{P_{M\min}(i)}{-i}, \quad \text{if } i < 0 \\ u_{col}(i) &= \frac{P_{M\max}(i)}{i}, \quad \text{if } i \geq 0 \end{aligned} \tag{40}$$

They are the two branches of the hyperboles asymmetric with respect to the point 0 of the coordinate system.

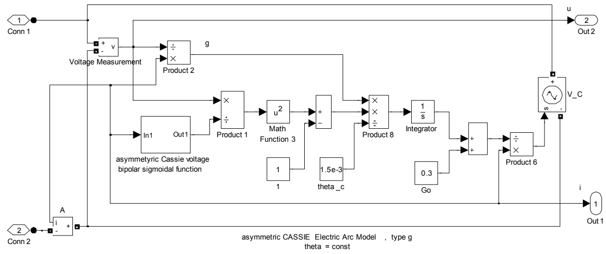

Fig. 1. Electrical asymmetric arc macro-model (10)

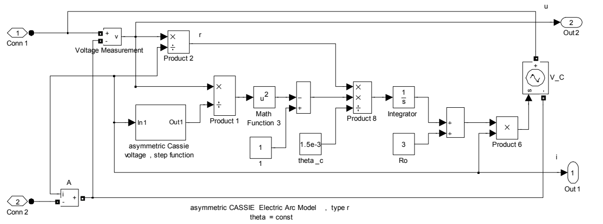

Fig. 2. . Electrical asymmetric arc macro-model (11)

a)

b)

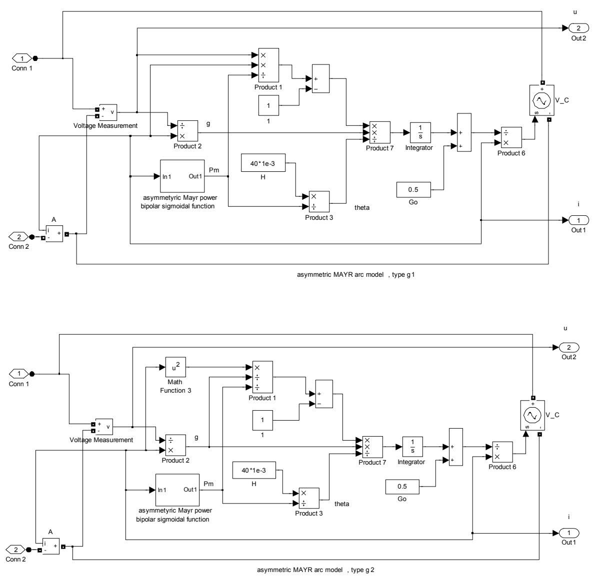

Fig. 3. . Electrical asymmetric arc macro-models representing the Mayr conductance-type models: a) Eq. (26); b) Eq. (27)

Power parameters of the Cassie and Mayr asymmetric Arc models

The Cassie and Mayr asymmetric arc models described above were implemented in the MATLAB-Simulink software. The diagrams of the relevant subsystems are shown in Figs. 1-4. The additional subsystems include the Cassie voltage approximating function [5] and the Mayr power approximating function [6]. They were used for simulating the non-steady states in arc circuits. Fig. 5 shows the hysteresis loop for the voltage $u_a(i)$ and power $p_a(i)$ of a system with asymmetric arc models: the Cassie type "g" model and the Mayr type "r" model, powered by a sinusoid voltage of frequency 50 Hz. The conductance models are fully equivalent to the corresponding resistance models. Additionally, the graph is shown representing the hysteresis loop for the momentary power p_{col} dissipated by the arc column. It is evident that in the case of short arcs a large portion of power is dissipated near the electrodes.

a)

b)

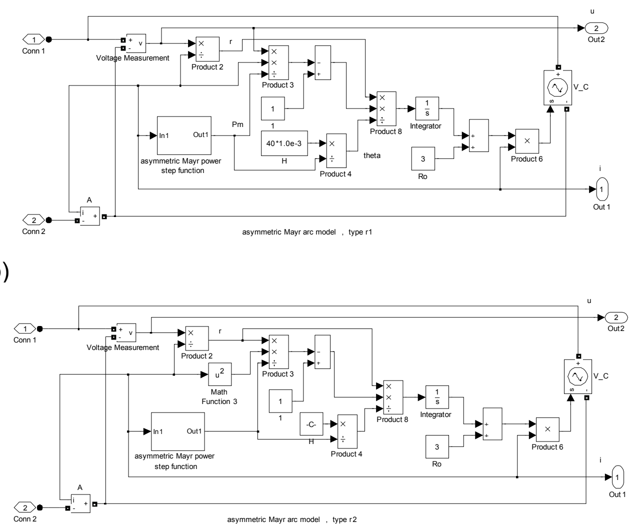

Fig. 4. Electrical asymmetric arc macro-models representing the Mayr resistance-type models: a) Eq. (28); b) Eq. (29)

a)

b)

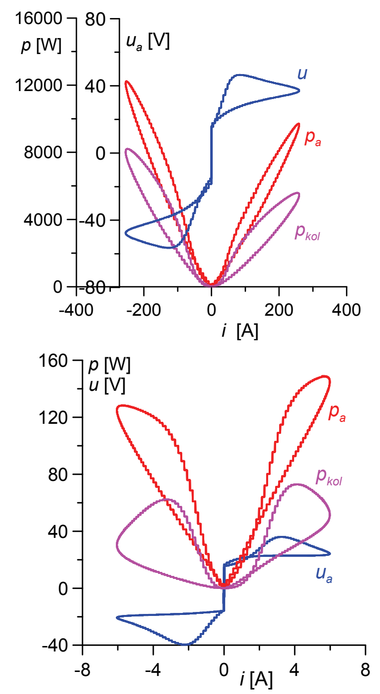

Fig. 5. Hysteresis loops for the voltage and power of the asymmetric arc models: a) Cassie type g (α=14V, U_{Cmin} = -30V, U_{Cmax} = 20V) ; b) Mayr type r (α=15V, P_{Mmin}=20W, P_{Mmax}=45W, H_0=4e-2J)

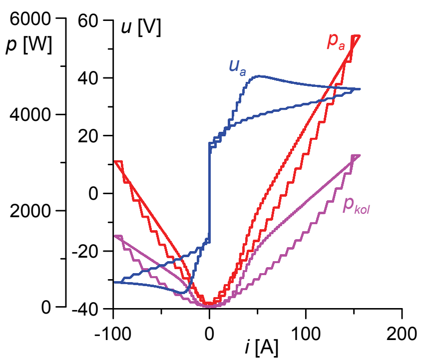

Fig. 6. Hysteresis loops for the voltage and power of the Cassie asymmetric arc model, type g (α=14V, U_{Cmin} = -30V, U_{Cmax} = 20V)

It was assumed in the paper that the arc distortions occur in steps which are asymmetric and synchronous with the current. The time waveforms of the distortions can, however, come in shapes other than rectangular or can appear synchronously with a subharmonic frequency. Taking this into account would require a modification of the arc macromodel.

An additional factor contributing to asymmetry of the waveforms is the non-alternating current forcing. Such modulated forcings are applied in plasma generators for welding in shielding gas atmosphere (e.g. MIG or TIG). Fig. 6 shows hysteresis loops for the voltage $u_a(i)$ and power $p_a(i)$ of the system with the Cassie asymmetric arc type „g", powered by meander-shaped voltage, of frequency 25 Hz, filling degree 30%, amplitude 200 V, and constant component -80 V.

Conclusions

1. On the basis of the qualitative assessment of the graphs $u(i)$ i $p(i)$ it can be stated that the dynamic characteristics of the dissipated power reflect the arc asymmetry in a significantly more adequate way than the voltage-current characteristics.
2. The arc models described in the paper can be successfully applied for simulating operating conditions of electrothermal and welding devices with a strong asymmetry of dynamic characteristics and with forced current of any type.

Praca naukowa finansowana przez MNiSzW ze środków na naukę w latach 2010-2013 jako projekt badawczy Nr N N511 305038.

REFERENCES

[1] *Plasmatechnik, Grundlagen und Anwendungen Eine Einfuhrung*, Carl Hanser Verlag, Munchen, Wien 1984
[2] Sawicki A., Asymetria charakterystyk dynamicznych łuku elektrycznego, *Śląskie Wiadomości Elektryczne*, No 4, 2010, 10-14
[3] Kruczinin A.M., Sawicki A., *Piece i urządzenia plazmowe*, Cz.2. WPCz, Częstochowa 2001
[4] Новиков О.Я., Тамкиви П.И., Тимошевский А.И. (eds.), *Многодуговые системы,* Наука, Новосибирск 1988
[5] Sawicki A., Modele Cassiego łuku asymetrycznego, *Śląskie Wiadomości Elektryczne,* No 4, 2010, 15-18
[6] Sawicki A., Modele Mayra łuku asymetrycznego, *Śląskie Wiadomości Elektryczne,* No 4, 2010, 19-22

***Author**: dr hab. inż. Antoni Sawicki, Politechnika Częstochowska, Instytut Elektroenergetyki, al. Armii Krajowej 17, 42-200 Częstochowa, E-mail: sawickia@el.pcz.czest.pl ;*